American Mineralogist, Volume 62, pages 79–88, 1977

Orientation relationships of augite exsolution lamellae in pigeonite hosts

H. NAKAZAWA AND S. S. HAFNER

Department of Geosciences, University of Marburg
3550 Marburg, Germany (F.R.G.)

Abstract

Pigeonite crystals ($Wo_{6-14}En_{56-64}Fs_{28-34}$) from lunar basalt 14053 were studied, using X-ray precession and Laue methods. Four distinct phases are generally present in each crystal: pigeonites P1, P2, and augites A_{001}, A_{100}. The orientation, relative intensity, and diffuse-streak relationships between the four phases indicate that there are two host-exsolution pairs, P1–A_{001} and P2–A_{100}, which correspond to two successive generations of exsolution at high and lower temperatures, respectively, during cooling. The presence of diffuse streaks connecting the reflections of P1–A_{001}, P2–A_{100}, and P1–P2 pairs suggests direct lattice interrelations of each pair.

The change of the plane of intergrowth from (001) to (100) is interpreted in terms of two-dimensional misfit between host and exsolved lattices, using published high-temperature data on clinopyroxenes. The temperature dependency of the calculated misfit ratios of the *a* and *c* axes show crossing over at a "critical temperature," above which the *a* axis yields the better fit, whereas the *c* axis fit is preferable below that point. The temperature dependency of the misfit ratios is consistent with two stages of exsolution of A_{001} and A_{100} above and below the critical temperature.

Because of the two generations of exsolution, the chemical compositions of the P1 and P2 hosts are expected to be somewhat different. The small differences in the lattice constants produce an apparent rotation of the c^* and a^* axes of the two hosts which can be recognized in precession photographs. The sense and magnitude of the rotation seems to depend on the change in chemical composition of the host resulting from the exsolved phase.

Introduction

Pyroxenes which have exsolved during cooling will be useful recorders of the cooling history of rocks if the crystallographic relationships of hosts and exsolved phases are fully understood. In the past few years, considerable efforts have been devoted to the problem of exsolution in pyroxenes, but many questions on nature and genesis are not yet resolved. Morimoto and Tokonami (1969), in a study of pigeonite crystals from the Moore County meteorite, suggested *simultaneous* exsolution of augite parallel to (001) and (100) planes of intergrowth. They assumed identical chemical composition in both types of augites and interpreted the observed small differences in the lattice constants (room-temperature values) numerically in terms of mechanical strain.

Smith (1969a), however, pointed out that at high temperatures (001) should be preferred as the plane of intergrowth over (100), because of minimum areal distortion at the temperature exsolution occurred. His reasoning implies two stages of exsolution with a switch of plane of intergrowth during cooling; consequently, different phases of exsolution with different chemical compositions result. Recent electron microscopic observations (Christie *et al.*, 1971; Nord *et al.*, 1973) seem to support this suggestion on a more empirical basis, pointing out a two-step sequence: "coarse augite and pigeonite lamellae form mainly along (001), which is followed by a fine tweed type exsolution in both phases."

Robinson *et al.* (1971) reconsidered the orientation of exsolution lamellae in pyroxenes and amphiboles from the point of view of the *O*-lattice theory of Bollmann and Nissen (1968). From a two-dimensional lattice fitting on the (010) plane, they concluded that "the lamellae are parallel to generally irrational planes of dimensional best fit between the lattices at the time exsolution began." Based on this argument, Jaffe *et al.* (1975) interpreted the optically observed angles of the "001" and "100" pigeonite

lamellae with respect to the c axis of host augites from the Adirondacks and elsewhere. Yet, it remained unclear "why ... the X-ray single crystal photographs show the lattices with their (001) planes essentially parallel" (Robinson *et al.*, 1971). No comment was made on the genesis of the (001) and (100) exsolution.

Several X-ray diffraction studies indicated a frequency correlation of exsolved (001) and (100) augite with the chemical composition of the pigeonite host; (100) augite is observed only in Mg-rich pigeonites (Takeda and Ridley, 1972) and in Ca-poor pigeonites (Takeda *et al.*, 1975).

In pigeonites from a lunar basalt (14053) of the Fra Mauro Formation, two crystallographically distinct host phases were detected which are related to two exsolved augite phases (Nakazawa and Hafner, 1975, Nakazawa *et al.*, 1976). This puzzling observation could not be interpreted in conventional terms of pyroxene exsolution. However, similar exsolution features can also be found in previously published X-ray precession photographs of pigeonites from different basalts. The two-host phenomenon seems to be a more general relationship in pyroxene exsolution history (Nakazawa and Hafner, 1976).

In this paper, some crystallographic details observed in pigeonite crystals from lunar basalt 14053 will be presented. To explain these observations, (001) and (100) exsolution based on the usual conception of lattice fitting will be discussed by use of high-temperature lattice data. This is along the line of Smith's suggestions in 1969. Finally, the observed crystallographic rotation between the two host lattices, which is believed to be consistent with the present reasoning, will be considered.

Experimental

Description of specimen

Rock chip 14053 is a basaltic fragment collected near the rim of Cone Crater at Fra Mauro on the moon. The rock is a coarse-grained holocrystalline basalt composed predominantly of clinopyroxene and plagioclase. The rock chip was crushed, sieved, and separated gravimetrically as described by Yajima and Hafner (1974) for basalt 15065. From the fraction with densities between 3.54 and 3.32 (grain size between 315 and 70 μm), about fifty magnesium-rich pigeonite crystals were hand-picked under the microscope for X-ray studies. All crystals were almost colorless or light honey-yellow. No obvious exsolution textures could be recognized optically, neither in the crushed crystal fragments nor in the thin section.

Average chemical composition

Electron microprobe analyses were made for about 30 crystal fragments in the same fraction from which crystals were chosen for the X-ray studies.

The pigeonite grains do not show any sign of chemical zoning, and their chemical variation from grain to grain is exceptionally small for clinopyroxenes from lunar basalts. It varies over the range Wo_{6-14} En_{56-64} Fs_{26-34} and is centered at $Wo_{11}En_{60}Fs_{29}$. For this separate, most crystal fragments appear chemically quite homogeneous (Nakazawa *et al.*, 1976).

X-ray studies

Crystal fragments with diameters between 70 and 120μm in average dimension were mounted with c^* parallel to a glass fiber. Precession photographs of $h0l$ and $0kl$ nets were taken, using a conventional camera (ϕ = 60 mm, Mo$K\alpha$ radiation with Zr filter). The cell dimensions of four coexisting phases measured for eight crystal fragments are given in Table 1. Laue photographs were also taken with the precession camera for some crystals with the same orientation as $h0l$ precession photographs: the incident beam was parallel to the b axis.

Orientation relationships, intensities, and diffuse streaks

Magnesium-rich pigeonite crystals from basalt 14053 show at least four distinct phases: two pigeonite hosts with space group $P2_1/c$ designated as P1 and P2, and two exsolved augites with space group $C2/c$, intergrown on (001) and (100) planes. The augites are designated as A_{001} and A_{100}, respectively. The two pigeonites have almost identical lattices with very similar orientations. The orientation relationships are as follows:

(1) The c^* axes of P1 and A_{001} are exactly parallel; the a^* axes are inclined to each other by about 2.7° ($=\Delta\beta_1$).

(2) The a^* axes of P2 and A_{100} are exactly parallel; the c^* axes are inclined to each other by about 2.9° ($=\Delta\beta_2$).

(3) The c^* axes of P1 and P2 are inclined to each other by about 0.4°, the a^* axes by about 0.3°.

(4) All four phases have the b axis in common.

The relative *orientations* of the four lattices may be recognized in Figure 1, which is a reproduction of the $h0l$ net of pigeonite crystal No. 51 with the typical P1–P2 splitting.

These relationships (1–4) indicate the existence of two related host-exsolution pairs, P1–A_{001} and P2–A_{100}, which imply successive generations of ex-

Table 1. Cell dimensions and estimated chemical compositions of two pigeonite hosts, P1 and P2, and two exsolved augites, A_{001} and A_{100}, coexisting in pigeonite crystals from basalt 14053.

Crystal number	Pyroxenes	a(Å)	b(Å)	c(Å)	β(°)	V(Å^3)	% of phase[a]	Nomogram composition[b] Wo	En	Fs
1	P1	9.68	8.91	5.21	108.6	425	10	5	62	33
	P2	9.64	8.91	5.22	108.7	425	60	4	63	33
	A_{001}	9.66	8.91	5.26	105.9	435	10	44	40	16
	A_{100}	9.73	8.91	5.22	105.6	436	20	49	37	14
2	P1	9.67	8.90	5.22	108.6	426	10	5	67	28
	P2	9.63	8.90	5.23	108.6	425	60	5	67	28
	A_{001}	9.68	8.90	5.27	105.8	437	10	47	40	13
	A_{100}	9.72	8.90	5.21	105.8	434	20	47	40	13
18	P1	9.67	8.89	5.20	108.6	423	60	5	68	27
	P2	9.66	8.89	5.23	108.7	424	20	3	70	27
	A_{001}	9.66	8.89	5.27	106.0	435	10	43	44	13
	A_{100}	9.74	8.89	5.21	105.8	434	10	46	42	12
21	P1	9.67	8.91	5.21	108.6	425	70	4	65	31
	P2	*[c]	*	*	*	*	5	*	*	*
	A_{001}	9.66	8.91	5.26	106.0	435	20	43	41	16
	A_{100}	*	*	*	*	*	5	*	*	*
22	P1	9.65	8.87	5.20	108.7	422	80	3	78	19
	P2	*	*	*	*	*	tr[d]	*	*	*
	A_{001}	9.65	8.87	5.25	106.0	432	20	44	48	8
	A_{100}	*	*	*	*	*	tr	*	*	*
23	P1	9.69	8.88	5.19	108.7	423	40	3	75	22
	P2	9.62	8.88	5.22	108.7	422	40	3	75	22
	A_{001}	9.64	8.88	5.27	106.1	433	10	42	48	10
	A_{100}	9.74	8.88	5.20	105.9	433	10	46	46	8
25	P1	9.74	8.88	5.20	108.6	426	70	5	72	23
	P2	*	*	*	*	*	5	*	*	*
	A_{001}	9.65	8.88	5.26	106.0	433	20	43	47	10
	A_{100}	*	*	*	*	*	5	*	*	*
51	P1	9.68	8.88	5.21	108.7	424	40	4	73	23
	P2	9.67	8.88	5.23	108.8	425	40	2	74	24
	A_{001}	9.67	8.88	5.27	105.9	435	10	45	45	10
	A_{100}	9.75	8.88	5.21	105.7	434	10	48	43	9

a) Volume ratios are roughly estimated from the intensity ratios of precession photographs.

b) Compositions estimated from b-β nomogram of Papike et al.(1971) were obtained by use of b and β values before rounding.

c) * indicates that the constant is not measured because of the uncertainty due to the diffuseness of the reflection. Estimated errors in cell dimensions are ±0.01 Å and ±0.1°.

d) tr : trace.

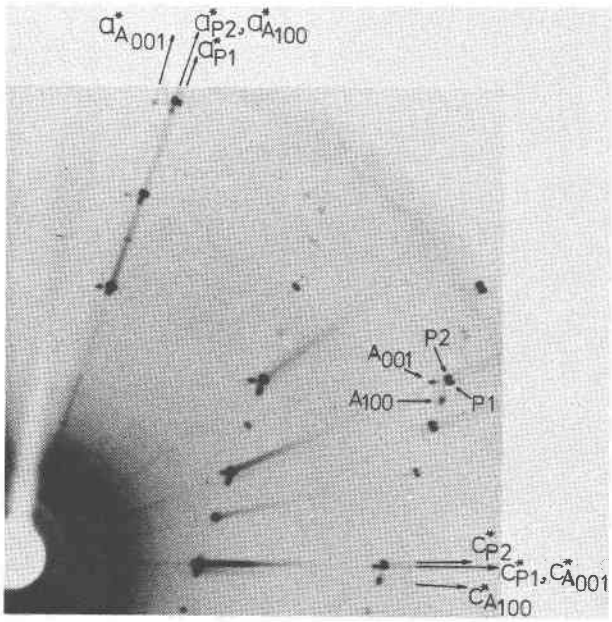

Fig. 1. Part of the *h0l* net of a precession photograph for a pigeonite crystal from basalt 14053 indicating the relationships between two pigeonite hosts and augite exsolved on (001) and (100) planes.

solution. The observation of two distinct host phases, P1 and P2, is of particular interest. Accidental disorientation of crystal fragments, epitaxis, or chemical zoning are excluded for the following reasons:

(1) Only the reflections of pigeonite show splitting.

(2) The double spots of pigeonite are generally connected by diffuse streaks.

(3) There are simple relationships involving the orientation, intensity, and diffuse streaks among the reflections of all four lattices as described later in more detail.

(4) All crystals studied exhibited similar diffraction patterns, which can also be recognized in crystals from other lunar basalts, *e.g.* in previously published precession photographs of Ghose *et al.* (1972, Fig. 2e, 2f) and Jagodzinski and Korekawa (1972, Fig. 10b).

(5) Electron microprobe analyses yielded no indication of chemical zoning within crystal fragments of the same separate.

The *intensities* of the four phases are interrelated. The P1 and P2 reflections are always stronger than those of their counterparts A_{001} and A_{100}. They are systematically correlated in that in different crystal fragments a relatively strong P2 reflection is coupled with a relatively strong A_{100} reflection, and a relatively weak P2 reflection is coupled with a relatively weak A_{100} reflection; a corresponding correlation applies also to P1 and A_{001}. The P1–A_{001} and P2–A_{100} pairs are undoubtedly exsolution pairs. Parts of *h0l* nets of some crystals (Nos. 38, 28, and 41) which show relative changes in the intensities of the pairs are presented in Figure 2.

The distinct reflections of the four phases are generally linked by *diffuse streaks*. In Figures 1 and 2a, diffuse streaks point from A_{100} spots toward the P2 spots along the a^* axis of P2. Yet in Figure 2b, they are smeared out between the P2 and A_{001} spots. In Figure 2c, the diffuse streaks seem to originate at the

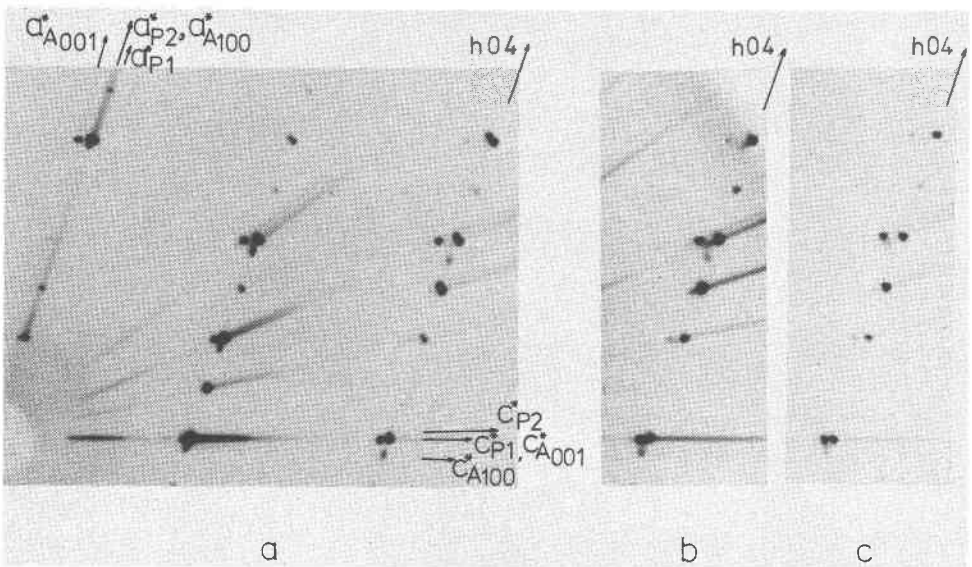

Fig. 2. Parts of *h0l* net of precession photographs for pigeonites from basalt 14053, indicating varying relative intensities between the two pairs of P1–A_{001} and P2–A_{100}.

A_{001} spots and point towards where the A_{100} reflection would occur, rather than vice versa. At any rate, a general trend of increasing diffuseness of P2 and A_{100} reflections may be recognized in Figure 2 from a to c. Using the argument that rates of atomic diffusion generally decrease with decreasing temperature, the comparatively more diffuse P2–A_{100} pair should be interpreted as representing the low-temperature exsolution pair which nucleated *after* the P1–A_{001} pair in the cooling process. Furthermore, the fact that $\Delta\beta_2 > \Delta\beta_1$ provides permissive evidence for the formation of the pair P1–A_{001} before P2–A_{100}, following the reasoning of Papike *et al.* (1971).

The two-dimensional diffuseness of the A_{100} reflections suggests that the A_{100} exsolution is not of the simple lamellae-type texture. The triangular diffuseness outlined by the limiting reflections of A_{001}, P2, and A_{100} as shown in Figures 2b and 2c may be indicative of a very early stage of exsolution with exceedingly small "lamellae." These fine-scale lamellae may eventually coarsen towards a more "mature" stage of exsolution as indicated by the features shown in Figure 1 and 2a.

Diffuse streaks may also be studied in Laue photographs. In Figure 3 a photograph of crystal No. 51 (same crystal as for Fig. 1) also illustrates the relative diffuseness of the P2–A_{100} pair with respect to P1–A_{001}. The figure shows clearly that diffuse streaks connect the spots of the host-exsolution pairs P1–A_{001} and P2–A_{100}, and also of the hosts P1 and P2. It should be noted that the A_{100} reflections in this crystal are exceptionally sharp. In all other crystals studied, they were more diffuse.

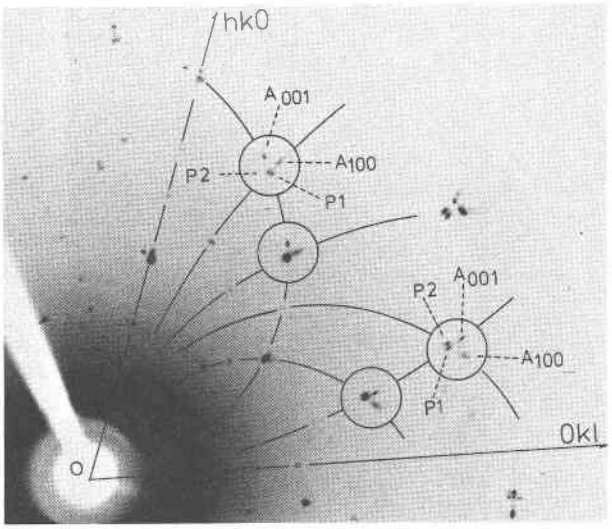

Fig. 3. Part of a Laue photograph of pigeonite from basalt 14053 indicating the diffuse streak relationships between the four clinopyroxene phases P1, P2, A_{001}, and A_{100}. The incident beam is parallel to the *b* axis, and some zones parallel to c^* and a^* are indicated. The crystal is the same as in Fig. 1.

Temperature-dependent fitting of host and exsolved lattices

The shared lattice planes

Recent optical studies of exsolution lamellae in metamorphic augites revealed that the phase boundaries of pigeonite exsolution lamellae are oriented on irrational planes near (100) and (001) (Jaffe *et al.*, 1975). The angular deviations of the "100" lamellae from ideal orientation varied between 0 to 22°, and those of "001" between 5 to 17°, depending on chemical composition. They were interpreted in terms of the optimal phase boundary theory (Jaffe *et al.*, 1975). From X-ray precession photographs, of course, no direct information is obtained on the boundary of host and exsolved phases. However, photographs show that the (001) or (100) *lattice planes* are essentially parallel (within less than 0.1 degree) as seen in Figure 1. Some clinopyroxenes of igneous and metamorphic origin exhibit a small angular "misorientation" of the c^* and a^* axes of host and exsolved lattices by some ten minutes. This discrepancy will be discussed at the end of this paper.

Moreover, Morimoto and Tokonami (1969) recognized that "the host and exsolved phases indicate two-dimensional agreement not only in orientation but also in cell dimensions along their boundary plane." Many more recently reported data on exsolved phases in pyroxene confirm this conclusion (*e.g.* Papike *et al.*, 1971; Prewitt *et al.*, 1971; Ghose *et al.*, 1972; Takeda and Ridley, 1972). This geometrical fitting relation is also correct for magnesium-rich pigeonite crystals from lunar basalt 14053. The cell edges *a* and *b* of P1 are quite close to the corresponding cell edges of A_{001}, and *c* and *b* of P2 to those of A_{100}. The observed lattice constants are presented in Table 1 together with estimated chemical compositions. In crystals from 14053, this simple concept of geometrical fitting is particularly obvious because of the well-resolved P1 and P2 phases. However, if the splitting of the host reflection is neglected, the resulting apparent misfit would be quite small, since the lattice dimensions of P1 and P2 are very similar.

This two-dimensional fitting between host and exsolved lattices suggests the presence of direct lattice interrelation between them, indicating that the shared planes of lattices are, at least approximately, the intrinsic (001) or (100) planes. Moreover, asymmetric

diffuse streaks are observed between the reflections of P1 and A_{001} along the c^* direction and between those of P2 and A_{100} along the a^* direction. These streaks do not indicate that the lamellae are extremely thin; however, they do imply the presence of some direct lattice interrelations between the intergrown phases. Therefore, we can restrict ourselves to (001) and (100) for further consideration of the lattice fitting of pyroxenes which show similar exsolution texture.

Two-dimensional fit of lattices at different temperatures

Since exsolution occurs at high temperatures, the two-dimensional fitting should be discussed by use of high-temperature cell-edge data. Moreover, the thermal expansion coefficient tensors should be known over the appropriate temperature range. Unfortunately, accurate high-temperature data within the pyroxene quadrilateral are scarce. However, with the data published so far, some semiquantitative estimates of the two-dimensional fit at high-temperatures may be made for clinopyroxenes of magnesium-rich composition.

It is well established that the b edges of pigeonite host and exsolved augite, and also of augite host and exsolved pigeonite, are parallel and of the same length, at least within the experimental error of the precession method. Exsolution, caused primarily by the segregation of calcium atoms, leaves the length of b nearly unchanged, as shown by the b–β nomogram of Papike *et al.* (1971), the b–$a\sin\beta$ nomogram of Brown (1960), or the b-composition diagram of Turnock *et al.* (1973). Moreover, b is the common axis for the (001) and (100) planes of intergrowth, which now will be considered. Therefore, inspection of the temperature dependence of a and c will reveal which plane, (001) or (100), is the plane of the better geometrical fit for an intergrowth of the two lattices.

In Figure 4 (left side), the literature values of a of selected clinopyroxenes are plotted against temperature. The thick lines, *A*, *D*, *a*, and *f*, correspond to the thermal variations of a for the compositions $Wo_5En_{95}Fs_0$ (Smith, 1969b; Stephenson *et al.*, 1966), $Wo_9En_{39}Fs_{52}$ (Brown *et al.*, 1972), $Wo_{50}En_{50}Fs_0$ and $Wo_{50}En_0Fs_{50}$ (Cameron *et al.*, 1973), respectively. In Figure 4 (right side) the same relationships are shown for c. Capital letters refer to $P2_1/c$ structures and lower case letters to $C2/c$ structures. The thin lines, *B*, *C*, *b*, *c*, *d*, and *e*, are interpolated, assuming a linear relationship from the thick lines for the respective compositions $Wo_6En_{73}Fs_{21}$, $Wo_8En_{61}Fs_{31}$, $Wo_{50}En_{43}Fs_7$, $Wo_{50}En_{36}Fs_{14}$, $Wo_{50}En_{23}Fs_{27}$, and $Wo_{50}En_{12}Fs_{38}$. The couples *B*–*b*, *C*–*c*, and *D*–*d* are almost those of the host and exsolution pairs according to the b–β nomogram by Papike *et al.* (1971). The

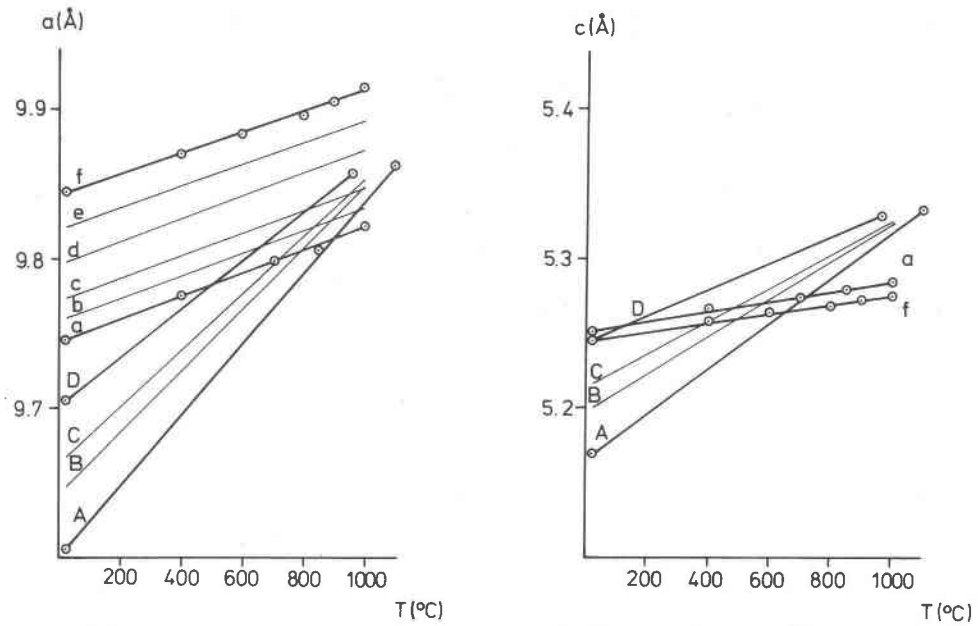

Fig. 4. Temperature dependence of lattice constants a (left) and c (right) for clinopyroxenes with different chemical compositions. The dots and thick lines indicate the measured lattice expansions, and the thin lines are interpolated. *A*: $Wo_5En_{95}Fs_0$; *B*: $Wo_6En_{73}Fs_{21}$; *C*: $Wo_8En_{61}Fs_{31}$; *D*: $Wo_9En_{39}Fs_{52}$; *a*: $Wo_{50}En_{50}Fs_0$; *b*: $Wo_{50}En_{43}Fs_7$; *c*: $Wo_{50}En_{36}Fs_{14}$; *d*: $Wo_{50}En_{23}Fs_{27}$; *e*: $Wo_{50}En_{12}Fs_{38}$; *f*: $Wo_{50}En_0Fs_{50}$. The interpolated lines of *b*, *c*, *d*, and *e* are between the lines of a and *f* of the right figure, but are not drawn in order to simplify the figure.

pigeonite from 14053 has an average chemical composition of $Wo_{11}En_{60}Fs_{29}$ and is almost on the tie-line of *C–c*. It should be borne in mind that the variations for pigeonites can not be linear as indicated in Figure 4, because of the inversion from the $P2_1/c$ to the $C2/c$ phase. Details will be discussed later in this section.

For convenience of illustration, "misfit ratios" are introduced and defined as the ratios *a*(pigeonite)/*a*(augite) and *c*(pigeonite)/*c*(augite). The dependence of the misfit ratios on the temperature for *B–b*, *C–c*, and *D–d* pairs are plotted in Figure 5. The solid parts of the lines in that figure indicate that part which exhibits the smaller geometrical misfit. The dashed vertical line marks a "critical temperature," *i.e.* the temperature where the crystallographic axis with the smaller misfit changes from *a* to *c* in cooling. Clearly, the (001) and (100) planes are the respective planes of the better geometrical fit above and below the "critical temperature." This simple geometrical relationship for the switch of planes from (001) to (100) is based entirely on mechanical strain energy.

The critical temperature obtained from the misfit ratios varies between 550 and 700°C, depending on chemical composition (*cf.* Fig. 5). That range of temperatures may be too low by 100°C or more, since a linear variation of the pigeonite lattice edges was used, neglecting the discontinuity at the $P2_1/c$ to $C2/c$ inversion. Smyth (1974) refined the crystal structure of a more iron-rich pigeonite ($Wo_2En_{31}Fs_{67}$) at several temperatures between 400 and 825°C. His data reveal *nonlinear* expansion coefficients for the *a* and *c* axes in that temperature range. If a corresponding, interpolated augite lattice (*e, cf.* Fig. 4) according to a tie-line from the nomogram of Papike *et al.* (1971) is used, a critical temperature of about 720°C is obtained. This temperature is about 120°C higher than that derived by using the simplified linear lattice expansion. Inspection of Smyth's data reveals that the critical temperature of his pigeonite is quite close to the temperature of inversion; the two temperatures may even be, in principle, the same. In that case, A_{001} is exsolved from the $C2/c$ (high-pigeonite) phase and A_{100} from the $P2_1/c$ (low-pigeonite) phase. Prewitt *et al.* (1971) indeed observed that "the *c*-axis of pigeonite is always about equal to or smaller than that of the (001) augite lamellae at room temperature, but expands to a value greater than that for augite *at the transition.*" More accurate data over a larger range of chemical composition in the pyroxene quadrilateral is necessary for further clarification.

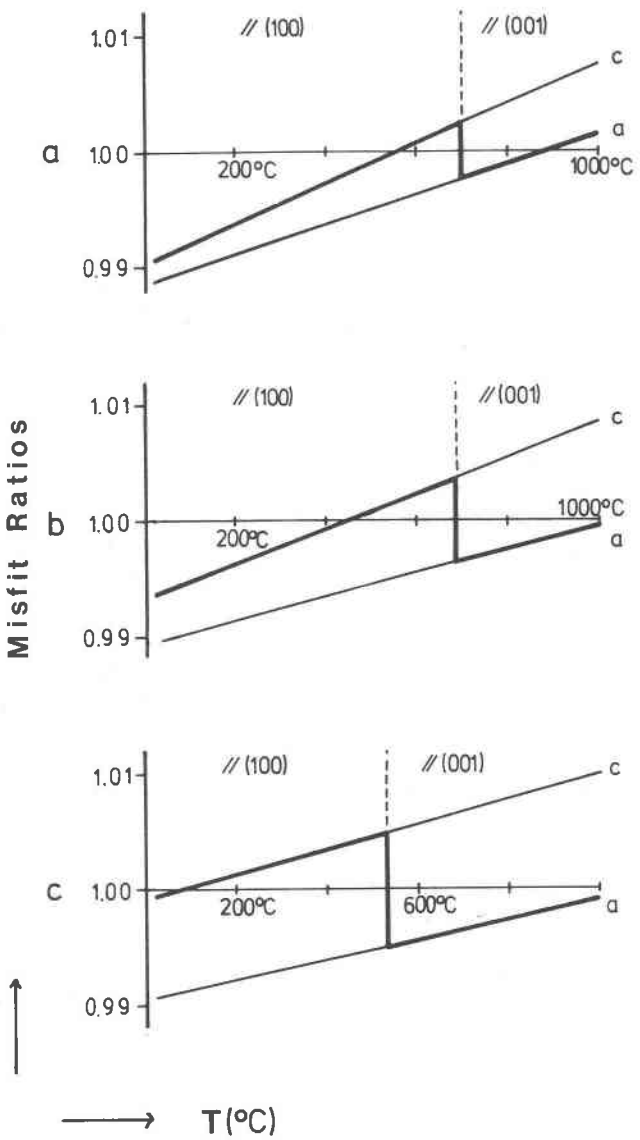

Fig. 5. Temperature dependence of the dimensional misfit ratios, for *B–b*, *C–c*, and *D–d* exsolution pairs. The solid parts of the lines represent the better fit axes. The vertical lines indicate the "critical temperatures" where the better fit axis changes from *a* to *c* in cooling. In view of the lack of accurate high-temperature lattice data, the straight lines should be considered as a rough approximation.

Apparent lattice rotation of host due to the second exsolution

As a consequence of the presence of metastable states in a simple, fairly rapid cooling process, the pigeonite host will be subjected to a subsequent change in chemical composition as augite is successively exsolved. The continual change of the host cell dimensions may be recognized in diffuse streaks that connect P1 and P2. The changes in the P1 and P2

lattices may be expressed in terms of an apparent rotation about the b axis.

Inspection of X-ray diffraction photographs of pigeonites from 14053 reveals that the splitting of reflections of the two pigeonite hosts is almost zero in a direction close to [$\bar{3}$01] (*cf.* Fig. 1, Nakazawa and Hafner, 1976). In fact, virtually the same interplanar distance for ($\bar{3}$01) is obtained when calculated from the P1 and P2 lattice constants at room temperature. The crystallographic relevance of this observation is not yet clear; the planes with identical spacings may be irrational. At any rate, the ($\bar{3}$01) plane may be used to define an apparent c^* and a^* rotation of the host lattices due to successive exsolution.

If the real and reciprocal lattice constants of the host before the beginning of exsolution are designated as a, c, a^*, and c^* (*cf.* Fig. 6), the small differences Δa, Δc, and $\Delta\beta$ indicate the change in the lattice which results from the change in chemical composition of the host during continued exsolution. Two directions of rotation should be noted: (i) $-\Delta a$, $+\Delta c$, $+\Delta\beta$, and (ii) $+\Delta a$, $-\Delta c$, $\pm\Delta\beta$ (*cf.* Fig. 6). Both directions appear to be possible. The direction indicated by (i) is the sense of rotation from P1 to P2 observed in magnesium-rich pigeonite from 14053. The opposite direction (ii) has been found, *e.g.*, in pigeonite from the Skaergaard intrusion (Morimoto and Tokonami, 1969, Fig. 3). A possible interpretation will be presented in the following section.

Discussion

X-ray observations of pigeonites from lunar basalt 14053 described in this paper are well understood by assuming *subsequent* (001) and (100) exsolution and relative rotation of the host due to the second, lower-temperature exsolution of augite A_{100}. They are in accord with recent phase diagrams in the pyroxene quadrilaterals (*e.g.* Ross *et al.*, 1973). For example, coarse augite and pigeonite lamellae form mainly along (001); they are followed by finer lamellae along (100), and this is indeed consistent with the change in the subsolidus curvature from high to low temperatures. The dependence of the frequency of (001) and (100) augite lamellae on chemical composition in pigeonite is also reasonably well understood: *e.g.* the rarity of the (100) exsolution in Fe-rich pigeonite may be due to a low critical temperture (*cf.* Fig. 5). A calcium-poor pigeonite from Mull ($Wo_{4.0}En_{40.5}Fs_{55.4}$) is an interesting special case which shows only A_{100} exsolution (Virgo and Ross, 1973). Here, there are

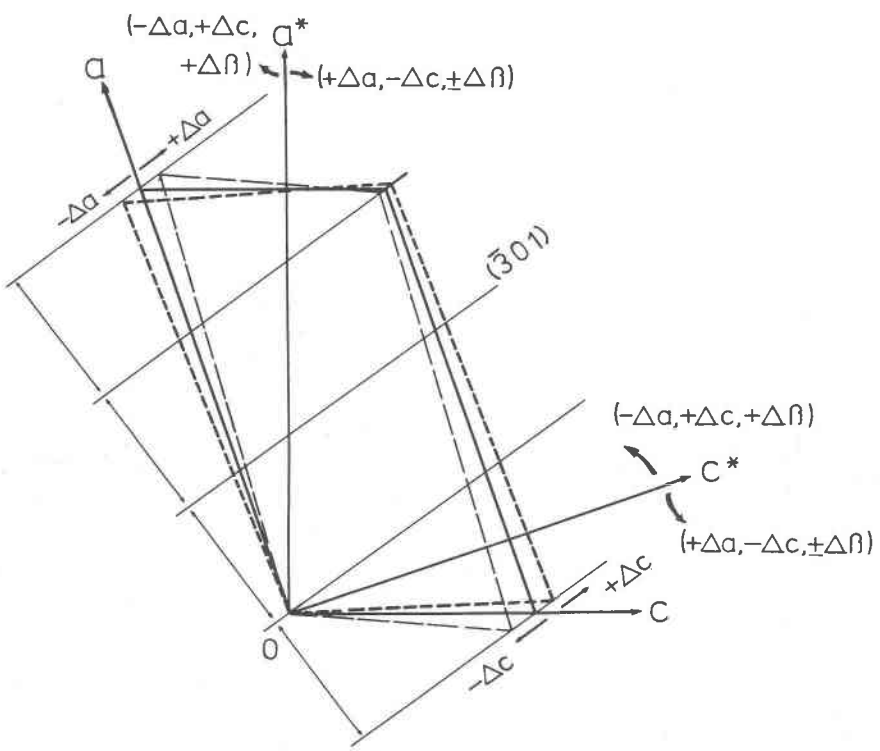

Fig. 6. Relative host lattice rotations due to the small changes of lattice constants, Δa, Δc, and $\Delta\beta$. The orientation of ($\bar{3}$01) plane remains unchanged, and its interplanar distance is the same. The arrows indicate the two directions of apparent rotation of the a^* and c^* axes.

two possible interpretations: pigeonite could not exsolve augite at high temperatures because of its composition, or it was rapidly cooled at high temperatures and slowly cooled, or annealed, at lower temperatures. Brown *et al.* (1972) found that a pigeonite of the bulk composition $Wo_9En_{39}Fs_{52}$ from the Mull locality exhibited faint exsolution on (001) and (100). This observation would rather support the first interpretation.

Our simplified model using misfit ratios should be considered as a first approximation only. Because of incomplete high-temperature lattice data, the nonlinear thermal expansion of pigeonites can not be appropriately accounted for. There are still some open questions. For example, the role of (001) exsolution lamellae in pigeonite (Ghose *et al.*, 1973) and augite (Robinson *et al.*, 1971) from metamorphic and plutonic rocks is not yet clear. However, the dependence of the c misfit ratios on temperature is generally stronger than that of a(*cf.* Fig. 5), and a crossing over of the ratios at quite low temperature may be possible. Thus, the a axis would again be the axis of the better fit.

The two-dimensionally diffuse reflections (*e.g.* 004), which represent initial stages of A_{100} exsolution, indicate intermediate orientations of the planes of intergrowth while changing from (001) to (100). Typically, the 004 reflection is diffuse within the triangular area outlined by the three positions of the P2, A_{001}, and A_{100} spots. This can be recognized clearly in pigeonite from lunar basalt 12040 (Ghose *et al.*, 1972, Fig. 2g). There, the 004 reflection of A_{001} seems to be almost vanishing (note that the relative lattice rotation of host pigeonite can be also seen in that figure). The two-dimensional diffuseness indicates that the exsolution texture is not of a simple lamellar type. The fine "tweed type" exsolution textures observed in electron micrographs (Christie *et al.*, 1971; Nord *et al.*, 1973) probably correspond to this kind of diffraction pattern; they are indicative of exsolution near the critical temperature. A theoretical treatment of the coherency of tweed type textures in X-ray diffraction would be interesting.

Some significant features of the relative lattice rotation of host pigeonite due to A_{100} exsolution can be recognized in some previously published precession photographs (*e.g.* Ghose *et al.*, 1972; Jagodzinski and Korekawa, 1972). Many details of the X-ray diffraction profiles are consistent with the present exsolution model, at least for some volcanic pigeonites (Nakazawa and Hafner, 1976).

High-temperature A_{001} lamellae in plutonic or metamorphic pigeonites are expected to exhibit a small, apparent "misorientation" with respect to the host lattice. In a very slowly cooled pigeonite, of course, the original host, with a composition close to P1, may be equilibrated completely by recrystallization to a new host, close to P2, with a somewhat different chemical composition corresponding to a lower-temperature range of the solvus. Therefore, the angle between the c^* axes of host and A_{001}, which may be defined as "misorientation" angle, may not necessarily reflect an intrinsic host exsolution relationship. It does not necessarily represent a real lattice rotation due, for example, to relaxation of strain (Morimoto and Tokonami, 1969), or to improving the fitting of irrational planes (Robinson *et al.*, 1971; Jaffe *et al.*, 1975). An intermediate stage of misorientation can be seen in the precession photograph of a pigeonite from soil south of Mare Crisium on the moon (Ghose *et al.*, 1973, Fig. 3). In that crystal, the 004 reflection of pigeonite is just a little elongated towards the $-a^*$ axis.

Pigeonites from Skaergaard (Morimoto and Tokonami, 1969) and Mare Crisium (Ghose *et al.*, 1973) reveal a lattice rotation in the opposite sense compared to pigeonites from volcanic rocks such as 14053. Thus, the 004 reflection of the host is rotated towards $-a^*$, yielding $+\Delta a$, $-\Delta c$, $\pm\Delta\beta$ according to Figure 6. Since the dependence of the lattice constants on chemical composition is monotonous (Turnock *et al.*, 1973), it is likely that an opposite change of lattice constants corresponds to an opposite change of the chemical composition. Such a rotation of the host lattice is caused by an exsolved phase with less calcium than the host. Actually, hypersthene ("inverted" pigeonite) is present in pigeonites from both localities. Therefore, opposite rotation of host pigeonite under special conditions might suggest exsolution of (not inverted) hypersthene simultaneously with, or subsequently to, A_{100} exsolution under rather equilibrated conditions.

Since the relative rotation of the host lattice is sensitive to the change of lattice constants which in turn depends on many factors, a detailed study on the basis of accurate lattice parameters at various temperatures is needed. Such a study should include a systematic analysis of the diffuse reflections.

Acknowledgments

We thank Dr. T. Yajima, Saitama University, for his mineral separation, Professor H. Jagodzinski, University of Munich, Professor M. Korekawa and Dr. L. Schröpfer, University of Frankfurt/Main, Dr. M. Ross, U.S. Geological Survey, and Dr. H. Takeda, University of Tokyo, for their kind interest and valuable

discussions. This work was supported by the Deutsche Forschungsgemeinschaft.

References

Bollman, W. and H. U. Nissen (1968) A study of optimal phase boundaries: the case of exsolved alkali feldspars. *Acta Crystallogr., A24,* 546–557.

Brown, G. E., C. T. Prewitt, J. J. Papike, and S. Sueno (1972) A comparison of the structures of low and high pigeonite. *J. Geophys. Res., 77,* 5778–5789.

Brown, G. M. (1960) The effect of iron substitution on the unit cell dimensions of the common clinopyroxenes. *Am. Mineral., 45,* 15–38.

Cameron, M., S. Sueno, C. T. Prewitt and J. J. Papike (1973) High-temperature crystal chemistry of acmite, diopside, hedenbergite, jadeite, spodumene, and ureyite. *Am. Mineral., 58,* 594–618.

Christie, J. M., J. S. Lally, A. H. Heuer, R. M. Fischer, D. T. Griggs and S. V. Radcliffe (1971) Comparative electron petrography of Apollo 11, Apollo 12 and terrestrial rocks. *Proc. 2nd Lunar Sci. Conf. (Geochim. Cosmochim. Acta Suppl. 2), 1,* 68–89.

Ghose, S., N. G. George and L. S. Walter (1972) Clinopyroxenes from Apollo 12 and 14: exsolution, domain structure, and cation order. *Proc. 3rd Lunar Sci. Conf. (Geochim. Cosmochim. Acta Suppl. 3), 1,* 507–531.

———, I. S. McCallum and E. Tidy (1973) Luna 20 pyroxenes: exsolution and phase transformation as indicators of petrologic history. *Geochim. Cosmochim. Acta, 37,* 831–839.

Jaffe, H. W., P. Robinson, R. J. Tracy and M. Ross (1975) Orientation of pigeonite exsolution lamellae in metamorphic augite: correlation with composition and calculated optimal phase boundaries. *Am. Mineral., 60,* 9–28.

Jagodzinski, H. and M. Korekawa (1972) X-ray investigations of lunar plagioclases and pyroxenes. *Proc. 3rd Lunar Sci. Conf. (Geochim. Cosmochim. Acta Suppl. 3), 1,* 555–568.

Morimoto, N. and M. Tokonami (1969) Oriented exsolution of augite in pigeonite. *Am. Mineral., 54,* 1101–1117.

Nakazawa, H. and S. S. Hafner (1975) Exsolution phenomena in clinopyroxene from basalt 14053 (abstr.). *Origin of Mare Basalt and their Implications for Lunar Evolution. Lunar Sci. Inst. Contrib. 234,* 111–114, The Lunar Science Institute, Houston.

——— and S. S. Hafner (1976) X-ray diffraction profiles and exsolution history of pigeonite. *Proc. 7th Lunar Sci. Conf. (Geochim. Cosmochin. Acta Suppl. 7),* in press.

———, A. El Goresy, S. S. Hafner and T. Yajima (1976) Pigeonite from basalt 14053: Chemistry and exsolution (abstr.). *Lunar Sci. VII* 604–606.

Nord, G. L. Jr., J. S. Lally, A. H. Heuer, J. M. Christie, S. V. Radcliffe, D. T. Griggs and R. M. Fisher (1973) Petrologic study of igneous and meta-igeneous rocks from Apollo 15 and 16 using high voltage transmission electron microscopy. *Proc. 4th Lunar Sci. Conf. (Geochim. Cosmochim. Acta Suppl. 4), 1,* 953–970.

Papike, J. J., A. E. Bence, G. E. Brown, C. T. Prewitt and C. H. Wu (1971) Apollo 12 clinopyroxenes: exsolution and epitaxy. *Earth Planet. Sci. Lett. 10,* 307–315.

Prewitt, C. T., G. E. Brown and J. J. Papike (1971) Apollo 12 clinopyroxenes: high temperature x-ray diffraction studies. *Proc. 2nd Lunar Sci. Conf. (Geochim. Cosmochim. Acta Suppl. 2), 1,* 59–68.

Robinson, P., H. Jaffe, M. Ross and C. Klein, Jr. (1971) Orientation of exsolution lamellae in clinopyroxenes and clinoamphiboles: consideration of optimal phase boundaries. *Am Mineral., 56,* 909–939.

Ross, M., J. S. Huebner and E. Dowty (1973) Delineation of the one atmosphere augite–pigeonite miscibility gap for pyroxenes from lunar basalt 12021. *Am. Mineral., 58,* 619–635.

Smith, J. V. (1969a) Crystal structure and stability of the $MgSiO_3$ polymorphs; physical properties and phase relations of Mg,Fe pyroxenes. *Mineral. Soc. Am. Spec. Pap., 2,* 3–29.

——— (1969b) Magnesium pyroxenes at high temperature: inversion in clinoenstatite. *Nature, 222,* 256–257

Smyth, J. R. (1974) The high temperature crystal chemistry of clinohypersthene. *Am. Mineral 59,* 1069–1082.

Stephenson, D. A., C. B. Sclar and J. V. Smith (1966) Unit-cell volumes of synthetic orthoenstatite and low clinoenstatite. *Mineral Mag., 35,* 838–846.

Takeda, H. and W. I. Ridley (1972) Crystallography and chemical trends of orthopyroxene–pigeonite from rock 14310 and coarse fine 12033. *Proc. 3rd Lunar Sci. Conf. (Geochim. Cosmochim. Acta Suppl. 3), 1,* 423–430.

———, M. Miyamoto, T. Isnii and G. E. Lofgren (1975) Relative cooling rates of mare basalts at the Apollo 12 and 15 sites as estimated from pyroxene exsolution data. *Proc. 6th Lunar Sci. Conf. (Geochim. Cosmochim. Acta Suppl. 6), 1,* 987–996.

Turnock, A. C., D. H. Lindsley and J. E. Grover (1973) Synthesis and unit cell parameters of Ca–Mg–Fe pyroxenes. *Am. Mineral., 58,* 50–59.

Virgo, D. and M. Ross (1973) Pyroxene from Mull andesites. *Carnegie Inst. Wash. Year Book, 72,* 535–540.

Yajima, T. and S. S. Hafner (1974) Cation distribution and equilibrium of pigeonite from basalt 15065. *Proc. 5th Lunar Sci. Conf. (Geochim. Cosmochim. Acta Suppl. 5), 1,* 769–784.

Manuscript received, May 17, 1976; accepted for publication, September 29, 1976.